

4-8-2021

Research on mechanism of bolt-grouting reinforcement for deep fractured rock mass based on prestressed anchor and self-stress grouting

Jin-peng ZHANG

College of Energy and Mining Engineering, Shandong University of Science and Technology, Qingdao, Shandong 266590, China

Li-min LIU

College of Energy and Mining Engineering, Shandong University of Science and Technology, Qingdao, Shandong 266590, China, llmsdust@163.com

Chuan-xiao LIU

College of Water Conservancy and Civil Engineering, Shandong Agricultural University, Tai'an, Shandong 271018, China

Dong-ling SUN

China Coal Technology Engineering Group Chongqing Research Institute, Chongqing 400037, China

See next page for additional authors

Follow this and additional works at: <https://rocksoilmech.researchcommons.org/journal>



Part of the [Geotechnical Engineering Commons](#)

Custom Citation

ZHANG Jin-peng, LIU Li-min, LIU Chuan-xiao, SUN Dong-ling, SHAO Jun, LI Yang, . Research on mechanism of bolt-grouting reinforcement for deep fractured rock mass based on prestressed anchor and self-stress grouting[J]. Rock and Soil Mechanics, 2020, 41(11): 3651-3662.

This Article is brought to you for free and open access by Rock and Soil Mechanics. It has been accepted for inclusion in Rock and Soil Mechanics by an authorized editor of Rock and Soil Mechanics.

Research on mechanism of bolt-grouting reinforcement for deep fractured rock mass based on prestressed anchor and self-stress grouting

Authors

Jin-peng ZHANG, Li-min LIU, Chuan-xiao LIU, Dong-ling SUN, Jun SHAO, and Yang LI

Research on mechanism of bolt-grouting reinforcement for deep fractured rock mass based on prestressed anchor and self-stress grouting

ZHANG Jin-peng^{1,2}, LIU Li-min², LIU Chuan-xiao¹, SUN Dong-ling³, SHAO Jun³, LI Yang²

1. College of Water Conservancy and Civil Engineering, Shandong Agricultural University, Tai'an, Shandong 271018, China

2. College of Energy and Mining Engineering, Shandong University of Science and Technology, Qingdao, Shandong 266590, China

3. China Coal Technology Engineering Group Chongqing Research Institute, Chongqing 400037, China

Abstract: To solve the problem of grout-rock interface relaxation due to self-shrinkage of cement-based material grouting in deep fractured rock masses, a bolt-grouting reinforcement method for deep fractured rock masses based on prestressed anchor and self-stress grouting was proposed. A self-stressed grouting reinforcement model and a new prestressed anchor rod-grouting reinforcement model for a single fractured rock mass were established. The mechanical characteristics of fractured sandstone specimens with ordinary and new bolt-grouting reinforcement were studied in physical experiments. The effectiveness of the new prestressed anchor rod-grouting reinforced rock mass was verified in engineering applications. Results showed that within a certain range, the greater the expansion restraint stress of the slurry stone is, the stronger the reinforcement effect on the fractured rock mass is. The expansion restraint stress of the slurry stone and the axial stress of bolt both contributed to the increase of the maximum principal stress of the fractured rock mass. The peak strength of the new prestressed anchor rod-grouting reinforced sandstone was 10% higher than that of the anchor rod-grouting reinforced sandstone. Its peak strain was slightly lower than that of the anchor rod-grouting reinforced sandstone. Moreover, the elastic deformation stage of the new prestressed anchor-grouting reinforced sandstone was shortened, and its reinforcement effect was enhanced. The surrounding rock of the substation roadway, which could not be well controlled by anchor-net support, U36 steel support or anchor rod-grouting reinforcement, was effectively controlled by new prestressed anchor rod-grouting reinforcement, and the maximum displacement of the surrounding rock on the roadway surface was 83 mm.

Keywords: fractured rock mass; prestressed anchorage; self-stressed slurry; bolt-grouting reinforcement; surrounding rock control

1 Introduction

Common methods for surrounding rock control include bolt net support, delayed grouting, steel support, shotcrete support, etc. Some experts and scholars have proposed various composite support methods for controlling surrounding rock under complex geological conditions^[1–3]. Bolt-grouting support is a typical kind of the composite support method, which combines advantages of prestressed anchor rod support and grouting reinforcement. The high geostress area, soft-rock roadway and the tunnel surrounding rock can be more effectively controlled by this composite support method than simple bolt support or grouting reinforcement^[4–8].

The main advantages of bolt-grouting to reinforce the broken surrounding rock of roadways include: (i) with the bolt-grouting reinforcement, the loose and broken surrounding rocks can be cemented as a whole and the cohesion, internal friction angle and strength of the rock mass are enhanced^[9–11]; (ii) Reinforced arch structures can be formed by the axial bolt reinforcement and the reinforcement of the grout diffusion, respectively, which expands the effective bearing range of the supporting structure, improves the integrity of the surrounding rock, and realizes the coordinated bearing of the sur-

rounding rock^[12–13]; (iii) when the grout seals the fractures of the rock mass, the internal structure of the rock mass is isolated from the external air, which can prevent air and water from entering the rock mass fractures and causing weathering or soaking^[14–16].

Some experts and scholars have conducted research on bolt-grouting reinforcement, which has achieved good reinforcement effects. Based on the test results of delayed grouting effect of deep soft rock roadway in Zhuji coal mine, Zhang et al.^[17] proposed a new type of support method combining shotcrete, bolt support and delayed grouting. Sun et al.^[18] used the scheme including both roadway floor anchor cable bundle and floor grouting in the south roadway of Taoer Mine^[18]. A concept of equivalent layer of bolt-grouting reinforcement was proposed by Meng et al.^[19]. Wang et al.^[20] put forward a new coupled bolt-grouting support technology with grouting anchor cable and grouting bolt as core. Zhai et al.^[21] comparatively studied the mechanisms of deformation and failure of roadway surrounding rock with bolt-shotcreting and bolt-grouting support in No.8 Mine, Pingdingshan. The combined support with prestressed anchor cables, shotcrete layer, bolt and metal net was proposed by Yu et al.^[22] when investigating the surrounding rock of the roadway of Mine II in Jinchuan. Moreover, Chen et al.^[23] presented a method

Received: 9 January 2020

Revised: 13 April 2020

This work was supported by the National Natural Science Foundation of China(51604164) and Shandong Province Key R&D Plan (2018GSF116006).

First author: ZHANG Jin-peng, male, born in 1992, PhD, Associate Professor, focusing on investigation of rock mechanics and grouting reinforcement. E-mail: zjpsdust@126.com

Corresponding: LIU Li-min, male, born in 1962, PhD, Professor, focusing on investigation of surrounding rock control and surface subsidence in underground engineering. E-mail: llmsdust@163.com

to enhance the rock bolting strength by introducing metal granules into the grouting material.

The grouting materials of bolt-grouting support mainly include cement-based grouting materials and chemical grouting materials. For chemical grouting materials, the setting time of can be easily controlled, but the strength is low, and the price is high. Additionally, some of the chemical grouting materials are poisonous. The cement-based materials are usually inexpensive and are relatively widely used in the field of rock engineering^[24–25]. The ground stress gradually increases, and geological conditions gradually become more complex with the increasing depth of underground engineering. As a result, the surrounding rock of the deep roadway after excavation is more and more broken. Due to poor fluidity and diffusibility of the cement-based grouting materials, it is difficult to completely fill the rock cracks, which greatly reduces the grouting reinforcement effect. Moreover, the self-shrinking property of the cement-based grouting materials caused by hydration can result in the slit between the grout stone body and the rock mass, which greatly reduce the effect of grouting reinforcement.

Although the expansion agents are used in the field of geotechnical engineering to reduce the self-shrinkage property of cement-based materials, it is relatively rarely applied in the field of rock mass grouting reinforcement. Due to the high stress constrained state of the deep rock mass, the expansion grout can increase the squeezing stress of the rock–grout interface through volume expansion in the fracture space, which can obviously enhance the shear strength of rock mass fractures. In addition, the reinforcement effect on the rock mass will be significantly improved because of the expansion stress of the grout stone body and the axial restraint stress of bolt acting together on the rock mass.

Therefore, to solve the problem of grout–rock interface relaxation due to self-shrinkage of cement-based material grouting in deep fractured rock masses, a bolt-grouting reinforcement method for deep fractured rock masses based on prestressed anchor rod and self-stress grouting was proposed in this study. The mechanism and application were investigated through theoretical analysis, physical experiment, field experiment and other methods. The admixture is used to promote the volume expansion of the grout stone body in the constrained space, which compensates for the self-shrinkage of the cement-based material and generates expansion stress at the same time. Thus, the restraint stress state and the bearing capacity of the reinforced rock mass are improved because of the expansion stress of the grout stone body and the axial restraint stress of bolt acting together on the rock mass.

2 Mechanical analysis of bolt-grouting reinforcement for fractured rock mass based on prestressed anchorage and self-stress grouting

2.1 Mechanical analysis of self-stress grouting reinforcement for a single fractured rock mass

The expansion agents are used to reduce the self-

shrinkage property of cement-based materials. The expansion agents can promote the volume expansion of the cement stone body to compensate for the self-shrinkage of the stone body. At present, the expansion agents are used mainly in the concrete-filled steel tube structure and for limiting the expansion rate of the concrete, and there are still limited studies for application in the grouting materials. When the amount of expansion agent exceeds the critical amount for compensating for the self-shrinkage of cement-based materials, the volume expansion of the grout stone body can not only compensate for the self-shrinkage of cement-based materials, but also can have a certain squeezing effect on the fracture wall in the confined space of the fractured rock mass. This squeezing stress can be regarded as the expansion stress. The expansion stress of the grout stone body acting on the fracture walls of the rock mass is caused by the volume expansion of the grout stone body in the constrained state. Therefore, this material is called self-stress grouting material. The main advantages of self-stress grouting reinforcement for rock mass are as follows: the stress state of the reinforced solid formed by the grout stone body and the rock mass is improved; in addition, the compactness and strength of the grout stone body are enhanced to a certain extent.

Some assumptions are made for a deep rock block: 1) it is in the original rock stress state, and there are restraint stresses acting on the rock block in the three-dimensional direction, σ_1 , σ_2 , σ_3 , respectively; 2) $\sigma_2 = \sigma_3$. There is a single fracture in the rock block, which is flat and has an infinitely small width. The angle between the direction of the fracture and the vertical direction is θ . According to the actual force state of the rock block, the restraints of the rock block in the two-dimensional direction are shown in Fig.1. There are elastic restraints for all the four corners of the rock block in the vertical and horizontal directions.

The self-stress grouting reinforcement for the fractured rock mass is carried out and the fracture is filled with expanding grouting materials. The expansion stress of the expanding grout stone body acting on the fracture wall in the constrained state is σ_s . The expansion restraint stress of the fracture wall on the grout stone body is σ_p . The vertical and the horizontal stress of the rock block is σ_1 and σ_2 , respectively. The mechanical model of self-stress grouting reinforcement for a single fractured rock mass is displayed in Fig.2.

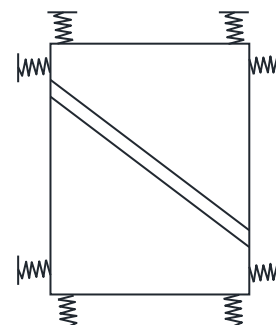


Fig. 1 Schematic diagram of the rock mass in the constrained state

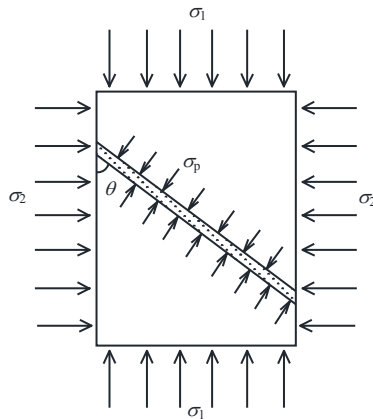


Fig. 2 Mechanical model of self-stress grouting reinforcement for a single fractured rock mass

Because the rock mass is in a state of deep high restraint stress, the expansion and compression stress of the grout stone body acting on the fracture wall only increase the compressive stress between the grout stone body and the fracture wall, instead of changing the overall restraint stress state of the rock mass. Therefore, the restraint force generated by the expansion stress is directed to the fracture wall.

The traditional sliding crack model is used for analysis of the self-stress grouting reinforcement of the single-fractured rock mass. The fracture surfaces slide against each other and the rock mass is destroyed under the action of vertical stress σ_1 and horizontal stress σ_2 on the single-fractured rock mass when the shear stress of the fracture surface exceeds the maximum shear strength between the fracture surfaces.

It is assumed in the sliding crack model that there is friction between the fracture surfaces of the compressive shear cracks in the compressed material, and the Mohr-Coulomb theory can be used for description of the friction and the normal stress between the fracture surfaces. In addition, other forces between the grout and the fractured surface of the rock mass such as bonding force also exist. The shear slip failure occurs in the fracture surface when the shear stress of the fracture surface can overcome the friction of the fracture surface and other forces between the grout and rock mass. The effective shear stress of the fracture surface is

$$\tau_{\text{eff}} = \tau_{xy} - f \tag{1}$$

$$f = \mu\sigma_n \tag{2}$$

where τ_{eff} is the effective shear stress; τ_{xy} is the shear stress on the fracture surface; f is the maximum friction of the fracture surface of the rock mass; σ_n is the normal stress on the fracture surface; and μ is the friction coefficient of the fracture surface.

Before the grouting reinforcement of the rock specimen is conducted, the normal stress on the fracture surface is

$$\sigma_n = \frac{1}{2}[(\sigma_1 + \sigma_2) + (\sigma_1 - \sigma_2)\cos(2\theta)] \tag{3}$$

$$\tau_{xy} = \frac{1}{2}(\sigma_1 - \sigma_2)\sin(2\theta) \tag{4}$$

With the self-stress grouting reinforcement, the direction of the expansion stress of the grout is parallel to the normal direction of the fracture surface, which points to the fracture wall. Therefore, the normal stress of the fracture wall is $(\sigma_n + \sigma_p)$ and the maximum friction is

$$f_1 = \mu(\sigma_n + \sigma_p) \tag{5}$$

where f_1 is the maximum friction of the fracture surface with the self-stress grouting reinforcement.

The effective shear stress of the fracture surface with the self-stress grouting reinforcement $\tau_{\text{eff}1}$ can be expressed as

$$\tau_{\text{eff}1} = \tau_{xy} - f_1 = \tau_{xy} - \mu(\sigma_n + \sigma_p) \tag{6}$$

The difference between the effective shear stresses without and with the self-stress grouting reinforcement Δ_1 is

$$\Delta_1 = \tau_{\text{eff}1} - \tau_{\text{eff}} = -\sigma_p\mu \tag{7}$$

Obviously, $\Delta_1 < 0$. Therefore, with the self-stress grouting reinforcement, the friction of the fracture surface increases, which leads to the decrease in the effective shear stress. The reduction of the effective shear stress of the fracture surface is $\mu\sigma_p$.

The criterion for the shear failure of the fracture surface is

$$\tau_{\text{eff}1} > \tau_c \tag{8}$$

where τ_c is the maximum shear strength of the fracture surface.

The self-stress grouting reinforcement for the fracture surface is carried out with the constant confining stress of the rock mass. The effective shear stress of the fracture surface decreases, and then the difference between the effective shear stress and the maximum shear strength of the fracture surface increases. A greater stress is needed to apply to make the effective shear stress reach the maximum shear strength.

Therefore, to make the effective shear stress of the fracture surface after self-stress grouting reinforcement reach the effective shear stress of the fracture surface before grouting reinforcement, it is necessary to increase the vertical stress of the rock block, which can be written as

$$\tau_{\text{eff}1} = \tau_{\text{eff}} \tag{9}$$

By solving Eq. (9), the vertical stress (σ_x) required to make the effective shear stress of the fracture surface reinforced by the self-stress grouting equals that not being reinforced by grouting can be obtained:

$$\sigma_x = \sigma_1 + \frac{\mu}{\cos\theta(\sin\theta - \mu\cos\theta)}\sigma_p \tag{10}$$

The increment in vertical stress Δ_2 is

$$\Delta_2 = \frac{\mu}{\cos\theta(\sin\theta - \mu\cos\theta)}\sigma_p \tag{11}$$

The relationship between σ_x and the expansion restraint stress σ_p according to Eq. (10) is plotted in Fig.3, in which K_p is the slope.

From Fig.3 it implies that after the rock block is reinforced by the self-stress grouting, the vertical stress

required to maintain the effective shear stress of the fracture surface equal to the effective shear stress before reinforcement is positively correlated with the expansion stress of the self-stress grouting material. The expansion stress of the grout stone body is relatively small compared to the initiation stress of the crack tip of the rock mass, therefore, it will not cause damage to the fracture of the rock mass, only have the restraint reinforcement effect on the rock mass. The greater the expansion restraint stress of the grout is, the greater the compressive stress required to cause shear slip failure on the fracture surface of the rock mass is. In other words, the greater the expansion restraint stress of the grout, the stronger the reinforcement effect on the fractured rock mass.

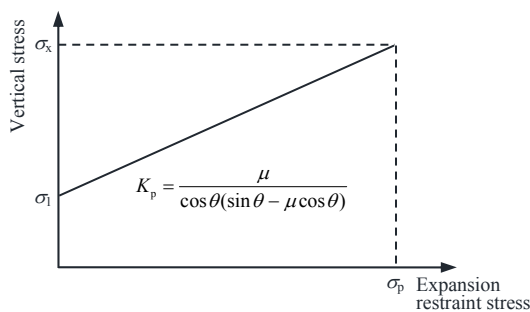


Fig. 3 Vertical stress required to maintain original effective shear stress after self-stressed grouting

2.2 Mechanism of the new prestressed anchor rod-grouting reinforcement

The self-stress grouting reinforcement can improve the mechanical parameters and the stress state of the rock mass. For the surrounding rock of a roadway, there is a free surface in the roadway after excavation. After the self-stress grouting reinforcement for the surrounding rock is carried out, the expansion stress on the fracture wall of the rock mass is produced by the grout. However, the surrounding rock on the surface is not constrained in the axial direction, and the constrained space required to generate the expansion stress may be displaced along with the expansion of the grout. Thus, the reinforcement effect of the self-stress grout cannot be achieved. Therefore, the prestressed grouting bolt is applied to restrain the surrounding rock of the roadway in the axial direction. The axial stress of the bolt limits the axial deformation of the surrounding rock, which can match the expansion stress caused by the self-stress grouting material on the fracture wall. The axial restraint stress of the prestressed anchor rod and the expansion stress of the self-stress grout on the rock mass contribute to an approximately three-dimensional strengthening state for the rock mass. Moreover, the prestressed anchor rods for the surrounding rock of the roadway are distributed in points rather than on planes. Therefore, the axial restraint stress of the rods on the rock mass is not uniform. This method involving both the prestressed anchor rod and the self-stress grout is called prestressed anchorage-grouting reinforcement. The new prestressed anchorage-grouting reinforcement model for a single fractured rock mass is displayed in Fig.4.

Assuming that the effect of the strength of the rod itself and shear resistance on the fractured rock mass is

not considered, the axial restraint stress of the anchor rod acting on the rock mass is uniformly distributed. σ_F is the axial stress of rod on rock mass, which increases the lateral stress of the rock mass σ_2 . Therefore, the maximum principal stress of the rock mass is enhanced. The restraint stress of the rock mass is changed, and the stress state of the rock mass is improved under the combined action of the axial restraint stress of the rod and the self-stress of the grout.

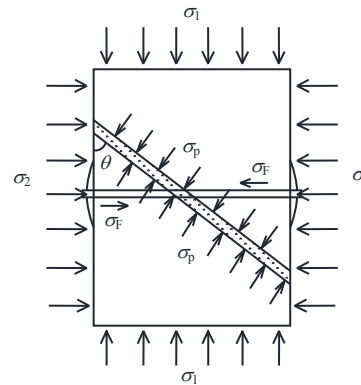


Fig. 4 New prestressed anchor rod-grouting reinforcement model for a single fractured rock mass

According to the superposition effect, the increment in the normal stress of the fracture surface in the rock mass by the self-stress grout is σ_p , which has no effect on the shear stress of the fracture surface. Additionally, the increment in the normal stress of the fracture surface of the rock mass by the rod is $\sigma_F \cos \theta$ and the increment in the confining pressure of rock specimens is σ_F . According to the above derivation, the normal stress, shear stress and effective shear stress of the fracture surface can be obtained when the self-stress grout and the anchor rod work together to strengthen the fractured rock mass:

$$\left. \begin{aligned} \tau_{\text{eff}2} &= \tau_{xy2} - \mu \sigma_{n2} \\ \tau_{xy2} &= \frac{1}{2} [\sigma_1 - (\sigma_2 + \sigma_F)] \sin(2\theta) \\ \sigma_{n2} &= \sigma_n + \sigma_p + \sigma_F \cos \theta \end{aligned} \right\} \quad (12)$$

where $\tau_{\text{eff}2}$, τ_{xy2} and σ_{n2} are the effective shear stress, the shear stress and the normal stress on the fracture surface, respectively when the fractured rock mass is strengthened by self-stressing grout and prestressed anchor rod simultaneously (i.e. prestressed anchor rod-grouting reinforcement).

Therefore, the effective shear stress $\tau_{\text{eff}2}$ of the fracture surface fractured rock mass reinforced by self-stressing grout and anchor rod simultaneously can be written as

$$\tau_{\text{eff}2} = \frac{1}{2} [\sigma_1 - (\sigma_2 + \sigma_F)] \sin(2\theta) - \mu (\sigma_n + \sigma_p + \sigma_F \cos \theta) \quad (13)$$

The difference between the effective shear stress by self-stressing grout and prestressed anchor rod simultaneously and the effective shear stress without being reinforced Δ_3 is

$$\Delta_3 = \tau_{\text{eff}2} - \tau_{\text{eff}} = - \left[\left(\frac{1}{2} \sin 2\theta + \mu \cos \theta \right) \sigma_F + \mu \sigma_p \right] \quad (14)$$

According to Eq. (14), when anchor rod-grouting method is used to reinforce the fractured rock mass, the reduction of effective shear stress on the fracture surface is greater than that when only a single reinforcement method is used to strengthen the fractured rock mass. The difference is the sum of the effective shear stress reduction with only self-stress grouting reinforcement and that with only anchor rod reinforcement.

When the prestressed anchor rod-grouting reinforcement for the fractured rock mass is carried out, the shear stress of the fracture surface can be reduced by increasing the lateral restraint stress of the fractured rock mass; at same time, increasing normal stress of the fracture surface can raise the friction force of the fracture surface, thereby reducing the effective shear stress on the fracture surface. The maximal shear strength of the fracture surface is related to the structural parameters of the fracture surface, which is constant without and with the prestressed anchor rod-grouting reinforcement. Consequently, the difference between the effective shear stress of the fracture surface with the prestressed anchor-grouting reinforcement and the maximum shear strength becomes larger. As a result, in order to make the effective shear stress of the fracture surface reach the maximum shear strength of the rock mass, a larger maximum principal stress must be required to cause the rock mass to fail. In other words, the shear strength of fractured rock mass strengthened by prestressed anchor rod-grouting is improved.

Assuming that the lateral stress of the rock mass remains constant, the effective shear stress of the fracture surface can reach the effective shear force without the prestressed anchor rod-grouting reinforcement under the action of the maximum principal stress:

$$\tau_{\text{eff}2} = \tau_{\text{eff}} \quad (15)$$

$$\tau_{\text{eff}2} = \frac{1}{2} [\sigma_x - (\sigma_2 + \sigma_F)] \sin(2\theta) - \mu \left[\frac{1}{2} (\sigma_x + \sigma_2) + \frac{1}{2} (\sigma_x - \sigma_2) \cos(2\theta) + \sigma_p + \sigma_F \cos \theta \right] \quad (16)$$

Solving Eq. (16) yields

$$\sigma_x = \sigma_1 + \frac{\mu}{\cos \theta (\sin \theta - \mu \cos \theta)} \sigma_p + \frac{\mu - \sin \theta}{\sin \theta - \mu \cos \theta} \sigma_F \quad (17)$$

The increasing amount of the vertical stress Δ_3 is

$$\Delta_3 = \frac{\mu}{\cos \theta (\sin \theta - \mu \cos \theta)} \sigma_p + \frac{\mu - \sin \theta}{\sin \theta - \mu \cos \theta} \sigma_F \quad (18)$$

Based on Eq. (18), both the grout expansion restraint stress and the axial stress of the anchor rod contributes to the increase of the maximum principal stress of the fractured rock mass, which can be expressed as

$$\left. \begin{aligned} \Delta_3 &= \Delta_2 + \Delta_4 \\ \Delta_2 &= \frac{\mu}{\cos \theta (\sin \theta - \mu \cos \theta)} \sigma_p \\ \Delta_4 &= \frac{\mu - \sin \theta}{\sin \theta - \mu \cos \theta} \sigma_F \end{aligned} \right\} \quad (19)$$

The slopes of the expansion stress of the grout, the axial stress of the anchor rod to the maximum principal stress required by the reinforced rock mass are K_p and K_F , respectively:

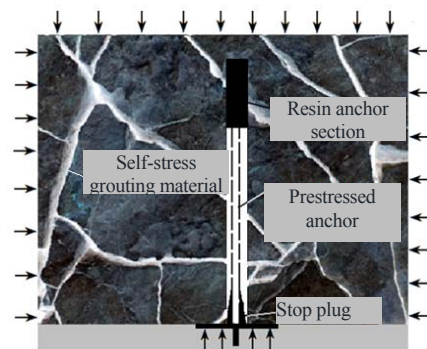
$$\left. \begin{aligned} K_p &= \frac{\mu}{\cos \theta (\sin \theta - \mu \cos \theta)} \\ K_F &= \frac{\mu - \sin \theta}{\sin \theta - \mu \cos \theta} \end{aligned} \right\} \quad (20)$$

K_p and K_F represent the sensitivity of the expansion stress of the grout to the maximum principal stress required by the reinforced rock mass, and the axial stress of the anchor rod to the maximum principal stress required by the reinforced rock mass, separately. According to Eq. (20), K_p and K_F are related to the friction coefficient of the fracture surface and the inclination of the fracture, and the friction coefficient of the fracture surface is influenced by the aperture, roughness, lithology, and other factors of the fracture surface.

The combination of self-stress grouting material and prestressed anchor rod-grouting support is a composite reinforcement method for fractured rock mass. It can not only significantly improve the stress state and the bearing capacity of the fractured surrounding rock, but also enhance the engineering reinforcement. Figure 5 shows the schematic diagram of anchor rod-grouting reinforcement based on prestressed anchorage and self-stress grouting.



(a) Before anchor rod-grouting



(b) After anchor rod-grouting

Fig. 5 Schematic diagram of anchor rod-grouting reinforcement based on prestressed anchorage and self-stress grouting

There are many advantages of anchor rod–grouting reinforcement based on prestressed anchorage and self-stress grouting:

(1) Recovery and improvement of the stress state of the rock mass

After the excavation of the roadway, it is necessary to recover the normal stress on the free surface of the roadway as much as possible within the shortest time and improve the stress state of the near-surface surrounding rock that is degraded by the roadway excavation. Through the axial restraint stress of the grouting anchor rod and anchor cable, and the expansion stress of the self-stress grouting material, the extrinsic strength and deformation modulus of the surrounding rock can be improved, and the tensile failure of the surrounding rock along the normal directions of the free surface and structural surface of the roadway can be limited.

(2) Strengthening and damage repair of the fractured surrounding rock area

The expansion stress of the self-stress grouting material can be generated during the condensation, which has the squeezing effect on the surrounding rock. The strength of the surrounding rock in the damaged and fractured area can also be recovered and enhanced, so that the surrounding rock in the fractured area caused by excavation disturbance can be effectively reinforced. Therefore, the initial three-dimensional stress state can be recovered as the state before excavation to a certain extent, and the strength of the reinforcement can be maximized.

(3) Enhancement of the inherent strength of rock mass

The loose and fractured surrounding rock turns to an overall dense surrounding rock because of the reinforcement of the prestressed anchor rod and the self-stress grout. The original state of the rock mass is restored to a certain degree and the self-bearing capacity of the surrounding rock is also improved. As a result, this can help with the stress release of the deep surrounding rock. Moreover, the inherent shear strength of the surrounding rock is enhanced, which limits the shear deformation of the surrounding rock along the potential fracture slip surface, and effectively improves the ability of the surrounding rock to resist shear failure under high stress. Overall, the axial restraint of the prestressed anchor and the lateral restraint of the self-stress grout are of great significance and value for the performance index which describes the strength enhancement of the reinforced rock mass.

3 Experiment and analysis of new prestressed anchorage–grouting

The effects of anchor rod –grouting reinforcement on fractured rock mass based on prestressed anchorage and self-stress grouting are investigated in physical experiments. Additionally, the prestressed anchor rod–grouting reinforcement of the rock mass are simulated by applying anchor rods in the horizontal direction of the grouting-reinforced rock specimen. By comparing the results of physical experiments and theoretical derivation, the correctness of the theory can be validated.

3.1 Experiment materials and methods

The rock material was sandstone taken from a coal

mine; the self-stress grouting material is composed of ultra-fine Portland cement and 10% expansion agent, in which the amount of the expander was obtained by experiment. The cement was #42.5 ultra-fine Portland cement produced by Shimen Cement Factory, which meets national inspection standards, and a U-type expander was used. Anchor rods purchased from a building material company were used for simulating the anchor rods as shown in Fig.6. In addition, the anchor tray was simulated with gaskets. Each bolt with a diameter of 4 mm is matched with two gaskets. The gasket has a thickness of 1.5 mm and a diameter of 10 mm. The flat gasket is made into a curved gasket by a plier with a certain angle parallel to the outer wall of the rock sample, which ensures that the gasket can fully contact the rock wall and the "protection" effect of the bolt tray can be simulated as displayed in Fig.7.



Fig. 6 Bolt for simulating the anchor rod

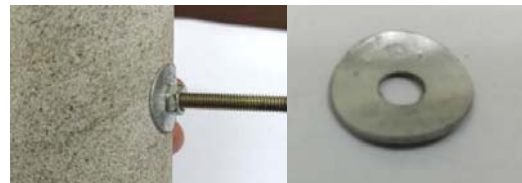


Fig. 7 Gasket for simulating the anchor tray

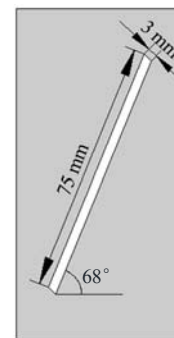


Fig. 8 Schematic diagram of prefabricated fractures in rock mass



Fig. 9 Constrained standard space trial model

First, a fracture was cut through the APW waterjet cutting system for a complete standard sandstone specimen with a width of 3 mm, an inclination angle of 68°, and a slit length of 76 mm. Then, the prefabricated

fractured sandstone was placed in a self-developed constrained standard space trial model, and ordinary grout and self-stress grout were injected, respectively. The ordinary grout wa ultra-fine Portland cement with a water–cement ratio of 0.45; the self-stress slurry consists of ultra-fine Portland cement and 10% U-type expansion agent with a water–cement ratio of 0.45. The grout was injected using a syringe into the fracture of the rock mass to ensure that the fracture was filled, and then the specimen was put into the constrained space standard trial mold (see Fig.9). Water was dripped into the slit of the test mold by a syringe to conserve the grouting stone body for 28 days. After this, the grouting reinforced specimen was taken out from the test mold. A hole of 5 mm diameter is generated transversely along the sample through the APW waterjet cutting system in the middle of the sample and it was far from the prefabricated fracture surface. The hole diameter is slightly larger than the bolt diameter, which can facilitate the bolt to play the role of axial restraint. Two gaskets matched with a bolt were respectively located at the two sides of the sample, and a certain pre-tightening force was applied to the bolt by tightening the nut with a plier, contributing to the effect of active anchoring. The nut of each rock specimen was screwed by the same person until it can no longer be rotated, so that the pre-tightening force applied on each rock specimen was approximately the same. In this test, the Shimadzu AG-X250 electronic universal testing machine was used to measure the mechanical properties of rock sample under the combined action of bolt anchoring and grouting reinforcement. The displacement loading control was used in the test with a loading rate of 0.01 mm/s.

3.2 Experiment scheme

The ordinary and self-stress grouting reinforced rock specimens were anchored by 0, 1, and 2 bolts. The bolt for the specimen with one bolt was located at the center, and the bolts were at the upper and lower 1/3 position of the specimen with two bolts. Each group of experiments were repeated 3 times. Additionally, the uniaxial compression tests for the ordinary and prestressed bolt-grouting reinforced specimens anchored by 0, 1, and 2 bolts were also analyzed. Figure 10 displays sandstone specimens anchored by one or two bolts.



Fig. 10 Sandstone specimens anchored by one or two bolts

3.3 Experiment result

3.3.1 Analysis of uniaxial compression test for the ordinary bolt-grouting reinforced fractured sandstone

The stress–strain curves of sandstone specimens with

the ordinary bolt–grouting reinforcement in the uniaxial compressive test are shown in Fig.11 and the failure mode of ordinary bolt–grouting reinforced sandstone specimens is presented in Fig.12.

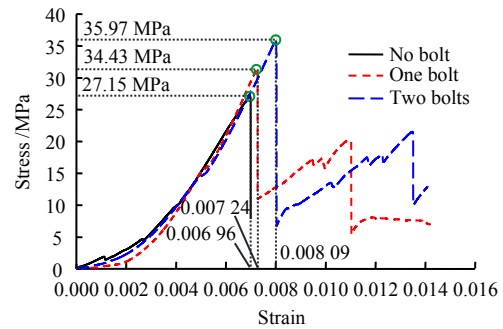


Fig. 11 Uniaxial compressive stress–strain curves of sandstone specimens with ordinary bolt-grouting reinforcement



Fig. 12 Failure mode of sandstone specimens with ordinary bolt-grouting reinforcement

Based on Fig.11, the ordinary grouting reinforced sandstone specimen anchored by no bolt undergoes the compaction stage, the elastic deformation stage before failure during the uniaxial compression test. Moreover, the ordinary grouting reinforced sandstone specimen anchored by one and two bolts goes through the compaction stage and the elastic deformation stage before reaching the peak strength. Then a delayed deformation is obviously witnessed after reaching the peak strength, and its bearing capacity increases to some extent at the later stage. It can be seen from Fig.12 that a certain shear slip failure first happens along the prefabricated fracture of sandstone specimens with the ordinary anchor-grouting reinforcement. However, the specimen can continue to bear the load due to the lateral restraint of the bolt. Then the fracture of the specimen continues to develop along the prefabricated fracture in the direction that is almost perpendicular to the end of the specimen, and the specimen is finally penetrated by the fracture. Because of the anchoring restriction of the bolt for the dilatancy of the specimen, there are bending and extension deformations for the bolt after failure.

The peak strength of sandstone specimens with the ordinary bolt–grouting reinforcement is obviously greater than that of sandstone specimens only with the ordinary grouting reinforcement. In addition, the peak strength of sandstone specimens with the bolt–grouting reinforcement anchored by one bolt and two bolts are 15.8% and 32.5% higher than that of the sandstone specimens with

the ordinary grouting reinforcement, respectively. The enhancement effect of a complete sandstone specimen with two bolts is obviously greater than that with only one bolt. Therefore, a higher anchoring strength of the sandstone specimen with the bolt–grouting reinforcement can contribute to a greater increase in the peak strength of the specimens.

The peak strain of sandstone specimens with the bolt–grouting reinforcement anchored by one bolt and two bolts are 4% and 16.2% larger than that of the sandstone specimens without the bolt reinforcement, respectively. This indicates that the bolt anchoring effect significantly extends the pre-peak deformation stage of the sandstone specimens with the ordinary grouting reinforcement. Moreover, the delay effect of two bolts on the failure of sandstone specimens with the ordinary grouting reinforcement is greater than that of one bolt.

3.3.2 Analysis of uniaxial compression test for the prestressed bolt–grouting reinforced fractured sandstone

The stress–strain curves of sandstone specimens with the prestressed bolt–grouting reinforcement in the uniaxial compressive test are shown in Fig.13 and the failure mode of prestressed bolt–grouting reinforced sandstone specimens is illustrated in Fig.14.

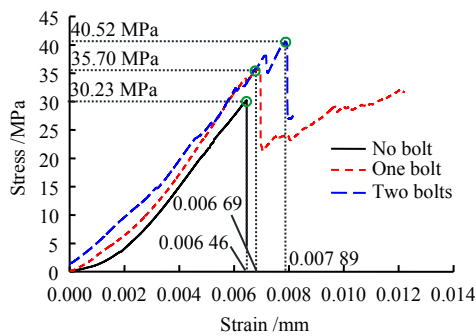


Fig. 13 Uniaxial compressive stress-strain curves of sandstones with prestressed bolt-grouting reinforcement



Fig. 14 Failure mode of sandstone specimens with prestressed bolt–grouting reinforcement

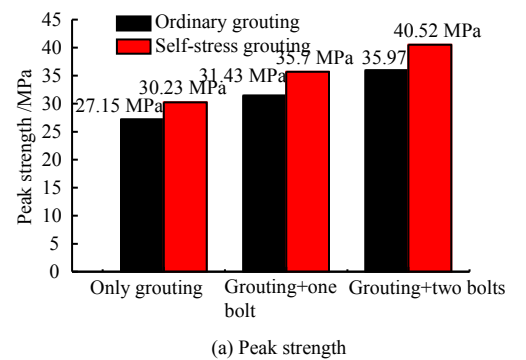
According to Fig.13, the change trend of the stress–strain curves of the self-stress grouting reinforced sandstone specimen anchored by zero, one and two bolts is similar to those of specimens with the ordinary grouting reinforcement, except that the values are different. Moreover, it can be observed from Fig. 14 that the failure mode of the sandstone specimen with the prestressed bolt–grouting reinforcement is also similar to that of the specimen with the bolt–grouting reinforcement.

The peak strength of sandstone specimens with the prestressed bolt–grouting reinforcement is obviously greater than that of sandstone specimens only with the self-stress grouting reinforcement. In addition, the peak strength of sandstone specimens with the prestressed bolt–grouting reinforcement anchored by one bolt and two bolts are 18.1% and 34% higher than that of the sandstone specimens with the self-stress grouting reinforcement, respectively. The enhancement effect of a complete sandstone specimen with two bolts is obviously greater than that with only one bolt. Therefore, a higher anchoring strength of the sandstone specimen with the self-stress grouting reinforcement can contribute to a greater increase in the peak strength of the specimens.

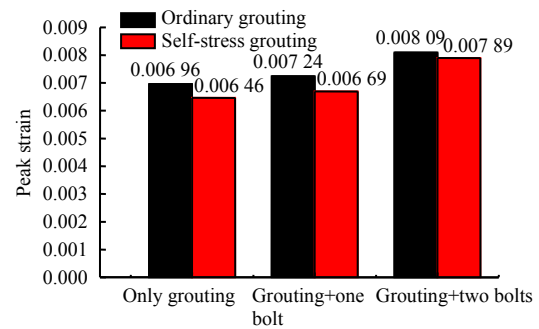
The peak strain of sandstone specimens with the prestressed bolt–grouting reinforcement anchored by one bolt and two bolts are 6.0% and 22.1% larger than that of the sandstone specimens only with the self-stress grouting reinforcement, respectively. This indicates that the bolt anchoring effect significantly extends the pre-peak deformation stage of the sandstone specimens with the self-stress grouting reinforcement. Moreover, the delay effect of two bolts on the failure of sandstone specimens with the self-stress grouting reinforcement is greater than that of one bolt.

3.3.3 Analysis and discussion

Under the action of the axial anchoring of the bolt and the expansion stress of the grout, the restraint stress of the reinforced rock mass is enhanced, further increasing its bearing capacity. In order to investigate the effect of the new prestressed bolt–grouting reinforcement, the peak strength and peak strain of the specimens with the ordinary and new prestressed bolt–grouting reinforcement are compared, as shown in Fig. 15.



(a) Peak strength



(b) Peak strain

Fig. 15 Peak strength and peak strain of sandstone strengthened by ordinary and prestressed bolt–grouting

According to Fig.15(a), for fractured sandstone specimens reinforced with only grouting, one bolt + grouting, and grouting + two bolts in each group, the peak strength of the specimens with the self-stress grouting reinforcement or prestressed bolt-grouting reinforcement is obviously greater than that of specimens with the ordinary grouting reinforcement or bolt-grouting reinforcement. The peak strength of the specimens with the self-stress grouting reinforcement is 11.34% greater than that of specimens with the ordinary grouting reinforcement. Additionally, the peak strength of the specimens with one-bolt and two-bolt prestressed bolt-grouting reinforcement is 13.59% and 12.65% greater than that of specimens with the bolt-grouting reinforcement, respectively. This illustrates that the prestressed bolt-grouting reinforcement has obvious advantages over the bolt-grouting reinforcement for fractured sandstone. With the self-stress of the grout stone body and the axial restraint stress of the anchor rod, the shear strength of the fracture of the rock mass crack is enhanced, and the overall bearing capacity of the specimen is also strengthened.

As displayed in Fig.15(b), the peak strain of the specimens with the self-stress grouting reinforcement is 7.18% smaller than that of specimens with the ordinary grouting reinforcement. Additionally, the peak strain of the specimens with one-bolt and two-bolt prestressed bolt-grouting reinforcement is 7.60% and 2.47% smaller than that of specimens with the bolt-grouting reinforcement, respectively. Therefore, the peak strain of the sandstone specimens with the prestressed bolt-grouting reinforcement is slightly smaller than that of specimens with the bolt-grouting reinforcement. However, the peak strength of the sandstone specimens with the prestressed bolt-grouting reinforcement is significantly greater than that of specimens with the bolt-grouting reinforcement. As a result, the elastic modulus of fractured sandstone specimens with the prestressed bolt-grouting reinforcement is significantly greater than that of specimens with the bolt-grouting reinforcement. The new prestressed anchor rod-grouting reinforcement can shorten the elastic deformation stage and have better reinforcement effects on the fractured sandstone specimens.

In this set of data, the sandstone with the prestressed bolt-grouting reinforcement has obvious advantages over the sandstone with the bolt-grouting reinforcement, which can also be found in the other two sets of test data.

The mechanism of the new prestressed anchor rod-grouting for improving the mechanical parameters of the fractured rock mass includes two aspects: on one hand, the restraint stress state can be formed by the self-stress of the grout and the axial restraint stress of the anchor rod acting on the rock mass; on the other hand, the strength and compactness of the grout stone body can be improved in a restraint state. The first aspect of the mechanism is theoretically analyzed above, while the second aspect should be investigated in physical experiments (SEM scanning), which will be further

discussed in our future work. Use of the new prestressed anchor rod-grouting reinforcement can greatly enhance the strength of the fractured rock mass and has better effects on the improvement and recovery of the strength of the fractured rock mass. The experiment results can well validate the mechanical advantages of the new prestressed anchor rod-grouting reinforcement in the theoretical part of Section 2. The specific application is carried out in Pingmei No.10 Mine to further investigate the effect of the new pre-stressed anchor rod-grouting on strengthening the rock mass through engineering practice.

4 On-site measurement

4.1 Project background

The ground elevation of -320 central substation in Pingmei No.10 Mine is +160–+185 m, and the underground elevation is -313–-314 m. Therefore, the buried depth of the roadway is 473–499 m. The roadway is located in the sandy mudstone, which is 0–4 m above the top of the W-8 coal seam. The rock layer above the sandy mudstone consists of 3–5 m fine-grained sandstone and 5–7 m medium-grained sandstone. Moreover, the roadway floor is composed of coal seams and 8–10 m sandy mudstone in sequence. Due to the high ground stress, the surrounding rock fractures are highly developed, and the rock layer is of lower hardness and has a greater degree of fracture. There are some fractures on the sides and top of the roadway of the substation. The peeling-off phenomenon and serious floor heave can also be witnessed. In order to ensure the normal power supply of the substation and safe production, the sides and floor of the substation need to be repaired. At present, the high strength anchor-net-cable support, U36 steel support or ordinary anchor rod-grouting reinforcement have been tried, but the roadway of the substation hasn't been well controlled. The damage of the roadway under the original support scheme is shown in Fig.16.



Fig. 16 Roadway damage under the original support scheme

4.2 Analysis of failure mechanism of the original support scheme

According to in-situ stress measurement data, the maximum principal stress at the -320 elevation measuring point is greater than 30 MPa. The maximum principal stress is almost along the horizontal direction with an average ratio of the maximum principal stress to the vertical stress of 1.99. This indicates that the tectonic stress in the mining area is relatively large, and it is the main stress affecting the stability of the surrounding rock. Therefore, although the buried depth of

the substation roadway is only around 500 m, it is still difficult to control the surrounding rock of the roadway.

①The U36 steel support is first applied in the roadway with a row spacing of 600 mm. Due to the large tectonic stress in the mine and the weak support for the surrounding rock of U36, the two sides are seriously deformed.

②Then, the high-strength anchor-net-cable support is used with the model of high-strength prestressed anchor rod $\Phi 20 \text{ mm} \times 2200 \text{ mm}$, and the row spacing is $700 \text{ mm} \times 700 \text{ mm}$; the model of the anchor cable is $\Phi 22 \text{ mm} \times 7300 \text{ mm}$, and the row spacing is $1400 \text{ mm} \times 400 \text{ mm}$. Though the supporting strength is relatively large, it is difficult to improve the self-bearing capacity of the surrounding rock only by high strength anchor cables because of the low strength of the sandy mudstone in the surrounding rock. Therefore, the surrounding rock cannot be well controlled.

③Later, bolt-grouting support is applied to control the surrounding rock, which has the same parameters same as the high strength anchor-net-cable support. The grouting anchor rod is of welding wire thread, and the ordinary cement grout is used. But the deformation of the roadway is still observed. This is because the anchor rod is mainly a grouting channel, with the extremely low prestress, which does not significantly restrict the surrounding rock in the axial direction. Additionally, the self-shrinking property of the ordinary cement can result in the slit between the grout stone body and the rock mass after solidification, and then the effect of grouting reinforcement is greatly reduced. Therefore, based on the above-mentioned lessons learnt from the failure of conventional surrounding rock control, prestressed anchor rods and self-stress grouting are applied in support for the substation roadway.

4.3 Prestressed anchor rod-grouting reinforcement scheme for roadway

According to the above research, a new prestressed anchor rod-grouting reinforcement method is used in the control test of the surrounding rock of a 50 m roadway of the substation. The design section of the new prestressed anchor rod-grouting support is shown in Fig.17, and the reinforcement parameters are as follows:

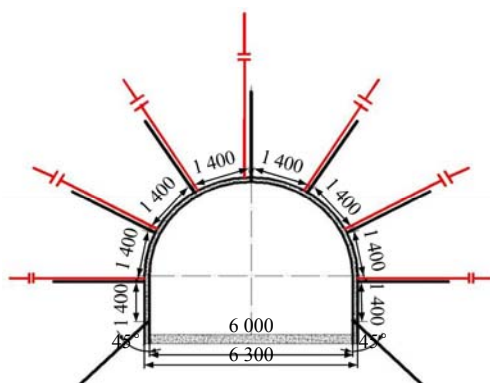


Fig. 17 Design section of new prestressed anchor rod-grouting support (unit: mm)

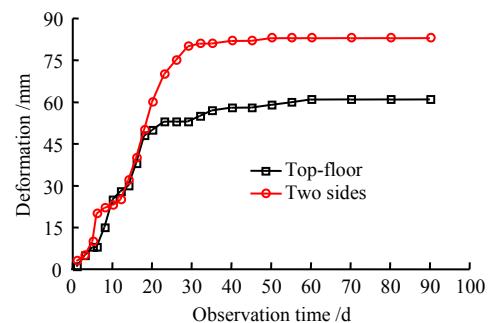
Anchor cable: the anchor rod is a new high-strength

prestressed grouting anchor rod with a wall thickness of 7 mm, and the model is $\Phi 25 \text{ mm} \times 2600 \text{ mm}$. It is made of fixed-rolled #45 steel seamless tube with a row spacing of $1400 \text{ mm} \times 1400 \text{ mm}$. In addition, the model of the anchor tray is $150 \text{ mm} \times 150 \text{ mm} \times 10 \text{ mm}$. One anchor rod is matched with one Z2835 resin anchoring agent, and the prestress is not smaller than 40 kN. The anchor cable is K22 grouting anchor cable, and its model is $\Phi 22 \text{ mm} \times 7300 \text{ mm}$. The row spacing is $1400 \text{ mm} \times 2000 \text{ mm}$. Moreover, the model of the anchor cable tray is $300 \text{ mm} \times 300 \text{ mm} \times 12 \text{ mm}$. One anchor cable is matched with two Z2835 resin anchoring agents, and the prestress is not smaller than 80 kN.

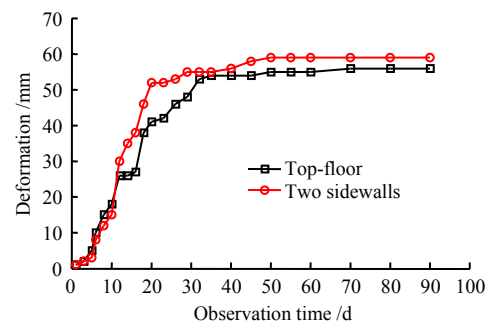
②Grouting material: self-stress composite grouting reinforcement material. The formula of this material is 79% of ultra-fine cement, 10% of expansion agent, 5% of clay, 6% of silica fume, and 5.4% of other additives. The water-cement ratio is 0.45 and the grouting pressure is not smaller than 4 MPa.

4.4 Deformation observation of surrounding rock of roadway

Six observation sections were selected in the roadway of the substation with the spacing of 10 m. The observation was made every 2 to 3 d at the initial stage and every 5 d at the later stage until the surrounding rock of the roadway was stable. The representative #2 and #4 observation points were selected for analysis. The deformation of top-floor and two sidewalls as a function of time is displayed in Fig.18.



(a) Deformation of the surrounding rock at 2# observation point



(b) Deformation of the surrounding rock at #4 observation point

Fig. 18 Curves of the deformation of top-floor and two sidewalls as a function of time

Based on Fig.18, the deformation of the two sidewalls of the roadway is obviously greater than that of the top and floor, which is consistent with the fact that the ground stress is dominated by horizontal stress. The

movement of the surrounding rock mainly occurs from 0 to 30 d. Although the deformation of the surrounding rock can be still observed after 30 d, the surrounding rock does not change a lot, and its deformation gradually stabilizes. After the stabilization, the maximum deformation of the top and floor of the roadway at observation points #2 and #4 are 61 mm and 56 mm, respectively, and the maximum deformations of the two sidewalls are 83 mm and 59 mm, respectively.

The surrounding rock of the substation roadway, which could not be well controlled by anchor–net–cable support, U36 steel support or ordinary anchor rod–grouting reinforcement, is effectively controlled by the new prestressed anchor rod–grouting reinforcement. The roadway is basically in a stable state with the maximum displacement of the surrounding rock on the roadway surface of 83 mm. The deformation of the surrounding rock is not large, and zero-repair after roadway repair is indeed realized. The substation roadway with new prestressed anchoring and grouting is shown in Fig.19. Therefore, the self-bearing capacity of the surrounding rock with the new prestressed anchor rod–grouting reinforcement can resist the stress release of the surrounding rock of the roadway.



Fig. 19 Substation roadway with new prestressed anchoring and reinforcement

5 Conclusions

(1) A anchorage–grouting reinforcement method for deep fractured rock masses based on prestressed anchor rod and self-stress grouting is developed. The admixture is used to promote the volume expansion of the grout stone body in the constrained space, which compensates for the self-shrinkage of the cement-based material and generates expansion stress at the same time. Therefore, the restraint stress state and the bearing capacity of the reinforced rock mass are improved because of the expansion stress of the grout stone body and the axial restraint stress of anchor rod acting together on the rock mass. The expansion restraint stress of the grout stone and the axial stress of anchor rod both contribute to the increase of the maximum principal stress of the fractured rock mass.

(2) The fractured sandstone with anchor rod–grouting reinforcement goes through the compaction stage and the elastic deformation stage before reaching the peak strength. Then a delayed deformation is obviously witnessed after reaching the peak strength, and its bearing capacity increases to some extent at the later stage. The specimen can still bear the load after reaching the peak strength due to the lateral restraint of the bolt and restriction on the dilatancy of the specimen. After failure,

bending and extension deformations can be observed for the bolt. A higher anchoring strength of the sandstone specimen with the bolt–grouting reinforcement can contribute to a greater increase in the peak strength of the specimens.

(3) The peak strength of the sandstone specimens with the prestressed bolt–grouting reinforcement is significantly greater than that of specimens with the ordinary bolt–grouting reinforcement. However, the peak strain of the sandstone specimens with the prestressed bolt–grouting reinforcement is slightly smaller than that of specimens with the ordinary bolt–grouting reinforcement. As a result, the elastic modulus of fractured sandstone specimens with the prestressed bolt–grouting reinforcement is significantly greater than that of specimens with the ordinary bolt–grouting reinforcement. Therefore, the new prestressed bolt–grouting reinforcement can shorten the elastic deformation stage and have better reinforcement effects on the fractured sandstone specimens.

(4) The surrounding rock of the substation roadway, which could not be well controlled by anchor–net–cable support, U36 steel support or ordinary anchor rod–grouting reinforcement, is effectively controlled by the new prestressed anchor rod–grouting reinforcement. The roadway is basically in a stable state with the maximum displacement of the surrounding rock on the roadway surface of 83 mm. Therefore, the self-bearing capacity of the surrounding rock with the prestressed anchor rod–grouting reinforcement can resist the stress release of the surrounding rock of the roadway.

References

- [1] WANG H, ZHENG P Q, ZHAO W J, et al. Application of a combined supporting technology with U-shaped steel support and anchor-grouting to surrounding soft rock reinforcement in roadway[J]. *Journal of Central South University*, 2018, 25(5): 1240–1250.
- [2] LI Gui-chen, SUN Hui, ZHANG Nong, et al. An investigation into shear stress distribution around hollow grouting anchor cables[J]. *Chinese Journal of Rock Mechanics and Engineering*, 2014, 33(Suppl.2): 3856–3864.
- [3] HAO Yu-xi, WANG Jiong, YUAN Yue, et al. Large deformation control technology for expansive and weak-cemented soft rock roadways in Shajihai coal mine[J]. *Journal of Mining & Safety Engineering*, 2016, 33(4): 684–691.
- [4] PAN Rui, WANG Qi, WANG Lei, et al. Research on mechanical effect and parameters of bolt-grouting reinforcement for deep roadway[J]. *Journal of Mining and Safety Engineering*, 2018, 35(2): 267–275.
- [5] SUN Li-hui, YANG Xian-da, ZHANG Hai-yang, et al. Experimental research on characteristics of deformation and failure of roadway ribs in soft coal seams under strong dynamic pressure and bolt-grouting reinforcement

- ment[J]. *Journal of Mining and Safety Engineering*, 2019, 36(2): 232–239.
- [6] ZHANG Mei-zhu, JIANG Quan, WANG Xue-liang, et al. Triaxial compression test and strengthening mechanism analysis of cracked marble specimens with bolting-grouting reinforcement[J]. *Rock and Soil Mechanics*, 2018, 39(10): 3651–3660.
- [7] WANG Q, JIANG Z H, JIANG B, et al. Research on an automatic roadway formation method in deep mining areas by roof cutting with high-strength bolt-grouting[J]. *International Journal of Rock Mechanics and Mining Sciences*. 2020, 128: 104264.
- [8] JIANG Bei, LI Shu-cai, WANG Qi, et al. Failure mechanism of three soft coal seam roadway and comparison study on bolt and grouting[J]. *Journal of China Coal Society*, 2015, 40(10): 2336–2346.
- [9] SHA F, LIN C, LI Z, et al. Reinforcement simulation of water-rich and broken rock with Portland cement-based grout[J]. *Construction and Building Materials*, 2019, 221: 292–300.
- [10] ZHANG J P, LIU L M, LI Q H, et al. Development of cement-based self-stress composite grouting material for reinforcing rock mass and engineering application[J]. *Construction and Building Materials*, 2019, 201: 314–327.
- [11] YU S F, WU A X, WANG Y M, et al. Pre-reinforcement grout in fractured rock masses and numerical simulation for optimizing shrinkage stoping configuration[J]. *Journal of Central South University*, 2017, 24(12): 2924–2931.
- [12] WANG Q, QIN Q, JIANG B, et al. Study and engineering application on the bolt-grouting reinforcement effect in underground engineering with fractured surrounding rock[J]. *Tunnelling and Underground Space Technology*, 2019, 84: 237–247.
- [13] WANG F T, ZHANG C, WEI S F, et al. Whole section anchor-grouting reinforcement technology and its application in underground roadways with loose and fractured surrounding rock[J]. *Tunnelling and Underground Space Technology*, 2016, 51: 133–143.
- [14] SHARMA K G, PANDE G N. Stability of rock masses reinforced by passive, fully-grouted rock bolts[J]. *International Journal of Rock Mechanics and Mining Sciences and Geomechanics Abstracts*, 1988, 25(5): 273–285.
- [15] LARBI S. Stability analysis of jointed rock slopes reinforced by passive, fully grouted bolts[J]. *Computers and Geotechnics*, 2001, 28(5): 325–347.
- [16] CHEN S H, FU C H, ISAM, SHAHROUR I. Finite element analysis of jointed rock masses reinforced by fully-grouted bolts and shotcrete lining[J]. *International Journal of Rock Mechanics and Mining Sciences*, 2009, 46(1): 19–30.
- [17] ZHANG Nong, WANG Bao-gui, ZHENG Xi-gui, et al. Analysis on grouting reinforcement results in secondary support of soft rock roadway in kilometre deep mine[J]. *Coal Science and Technology*, 2010, 38(5): 34–38.
- [18] SUN Li-hui, YANG Ben-sheng, SUN Chun-dong, et al. Experimental research on mechanism and controlling of floor heave in deep soft rock roadway[J]. *Journal of Mining & Safety Engineering*, 2017, 34(2): 235–242.
- [19] MENG Qing-bin, HAN Li-jun, QIAO Wei-guo, et al. Numerical simulation research of bolt-grouting supporting mechanism in deep soft rock roadway[J]. *Journal of Mining & Safety Engineering*, 2016, 33(1): 27–34.
- [20] WANG Lian-guo, LU Yin-long, HUANG Yao-guang, et al. Deep-shallow coupled bolt-grouting support technology for soft rock roadway in deep mine[J]. *Journal of China University of Mining and Technology*, 2016, 45(1): 11–18.
- [21] ZHAI Xin-xian, TU Xing-zi, LI Ru-bo, et al. Surrounding rock deformation mechanism of deep soft-rock roadway with bolt-grouting support[J]. *Coal Engineering*, 2018, 50(1): 36–41.
- [22] YU W J, WANG P, DU S H. Deformation mechanism of high-stress and broken-expansion surrounding rock and supporting optimization based on the gray correlation theory[J]. *Journal of Chongqing University (English Edition)*, 2014, 13(3): 99–114.
- [23] CHEN C, TING R, Cook C. Introducing aggregate into grouting material and its influence on load transfer of the rock bolting system[J]. *International Journal of Mining Science and Technology*, 2014, 24(3): 325–328.
- [24] AXELSSON. Mechanical tests on a new non-cementitious grout, silica sol: a laboratory study of the material characteristics[J]. *Tunnelling and Underground Space Technology*, 2005, 21(5): 554–560.
- [25] WANG De-ming, ZHANG Qing-song, ZHANG Xiao, et al. Research and application on tunnel and underground engineering grouting effect of the fuzzy evaluation method[J]. *Chinese Journal of Rock Mechanics and Engineering*, 2017, 36(Suppl.1): 3431–3439.
- [26] MENG Qiang, ZHAO hong-bo, RU Zhong-liang, et al. Analytical solution for circular tunnels with rock bolts[J]. *Engineering Mechanics*, 2015, 32(7): 18–23.